Electronic Supplementary Material (ESI) for Physical Chemistry Chemical Physics.

Electronic Supplementary Information (ESI) for: 'Isomerisation of an intramolecular hydrogen-bonded photoswitch: protonated azobis(2-imidazole)'

James N. Bull, Michael S. Scholz, Neville J. A. Coughlan and Evan J. Bieske

Synthetic procedure

Synthesis of azobis(2-imidazole) followed the procedure of Weston *et al.*[1] using AR grade reagents purchased from Sigma-Aldrich. Briefly, 2-nitroimidazole (100 mg) and potassium carbonate (174 mg) were suspended in acetonitrile (1 mL). Methyl iodide (66 μL) dissolved in 0.35 mL acetonitrile was added slowly while stirring at room temperature. The mixture was heated to 60°C for three hours. The reaction was quenched by addition of 1.4 mL water. Acetonitrile was removed *in vacuo*, the solution was diluted with a further 1.2 mL water, and the product extracted using four washes of ethyl acetate (3 mL). The combined organic phases were dried over anhydrous magnesium sulphate and concentrated to give crude 1-methyl-2-nitroimidazole, which was used without further purification. The 1-methyl-2-nitroimidazole product was dissolved in 5 mL of 0.1 mol aqueous ammonium chloride. Next, $\sim$10 mg zinc powder was added slowly with vigorous stirring to form a yellow coloured solution. The solution was heated at 45°C for an hour during which the solution turned orange in colour. The orange solution was diluted with 15 mL water and extracted with four 20 mL washes of chloroform, which were combined, dried over magnesium sulphate, and concentrated to yield azobis(1-methyl-2-imidazole) as an orange coloured powder.

E and *Z* isomers of PABI

Each of the three bonds linking the two heteroarene groups of PABI can have *E* and *Z* configurations giving a total of eight possible isomers. However, potential energy surface scans revealed only seven isomers (four *E* and three *Z*) are stable. These seven isomers along with the lowest energy isomerisation transition states (TS) are shown in Fig. S1. All ΔE values are relative to the energy of *E*1, the most stable isomer. The *E*4 and *E*3 isomers should relax to the more stable *E*1 and *E*2 isomers over relatively low isomerisation barriers whose height is below the estimated thermal energy at 300 K ($\approx$40 kJ mol^{-1} from the vibrational partition function of *E*1-PABI). The *E*1 and *E*2 isomers, which are separated by a more substantial barrier, are predicted to have similar collision cross sections and electronic spectra, and are likely to be indistinguishable in our experiments.

For the *Z*-isomers, only *Z*1 is expected to be present in the drift region as the *Z*2 isomer will rapidly convert to *Z*1 over a low isomerisation barrier (only 7 kJ mol^{-1} relative to *Z*2), while *Z*3 lies much higher in energy and will be thermodynamically disfavoured.

The *E*1-*Z*1 isomerisation barrier is $\approx$130 – 140 kJ mol^{-1} (see manuscript), depending on the inversion or torsion mechanism, which are much higher than any of the barriers in Fig. S1.

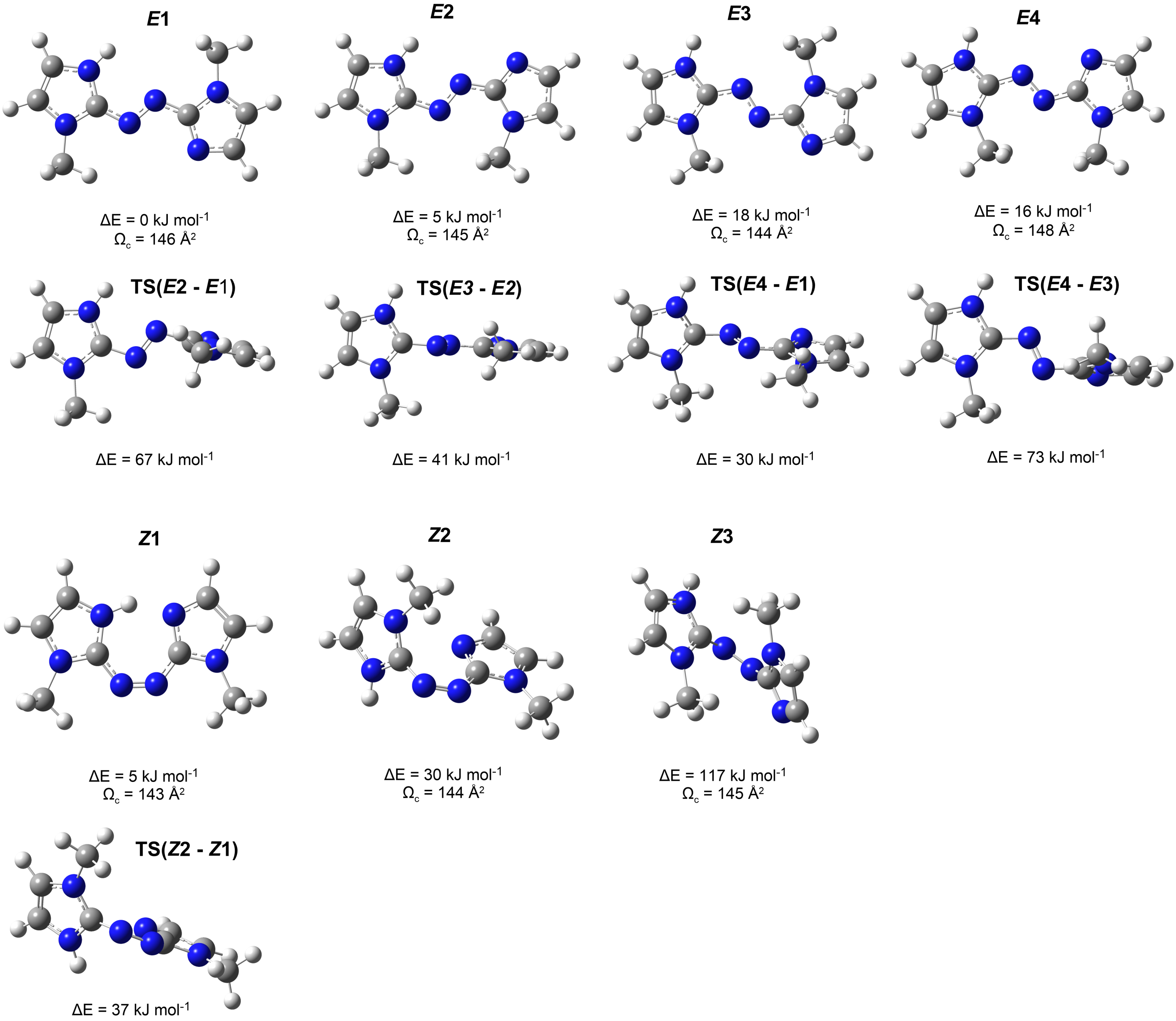

Fig. S1 *E* and *Z* isomers of PABI, and selected transition states (TS). ΔE values, given relative to *E*1, are at the DLPNO-CCSD(T)/cc-pVTZ/ωB97X-D/cc-pVTZ level of theory. Ω_c are calculated collision cross-sections.

Evaluation of the level of theory

This section justifies our choice of the level of electronic structure theory. Table S1 summarises calculated energies for *Z*1-PABI relative to *E*1-PABI. For both protonated cation and neutral couples, the CCSD(T)/cc-pVTZ/MP2/cc-VTZ value is considered the benchmark. As shown in Table S1, ωB97X-D slightly underestimates the relative energy. MP2 predicts the *Z*1-isomer to be more stable than the *E*1-isomer and CCSD overestimates the energy of the *E*1-isomer; both results suggest electron correlation is not properly described. Also included in Table S1 are values obtained using the DLPNO-CCSD(T) method with the 'standard cutoff' (as implemented in ORCA 3.0.3)[2] and 'tight cutoff' (values TCutPNO=1e-7, TCutPairs=1e-5, and TCutMKN=1e-4) truncation of the pairwise natural orbital virtual space.[3–5] The 'tight cutoff' criterion incorporates increased long-range correlation contributions to bring the calculation closer to the canonical CCSD(T) limit. The DLPNO-CCSD(T) method with the 'tight cutoff' criterion performs reliably compared with CCSD(T).

For the *E*-azonium isomer, ΔE calculated at the DLPNO-CCSD(T)/cc-pVTZ/ωB97X-D/cc-pVTZ level of theory is 66 kJ mol^{-1}, in excellent agreement with the CCSD(T)/cc-pVTZ value of 67 kJ mol^{-1}. Both ωB97X-D and MP2 methods underestimate ΔE at 60 kJ mol^{-1} and 42 kJ mol^{-1}, respectively.

Level of theory	ΔE(cation) / kJ mol^{-1}	ΔE(neutral) / kJ mol^{-1}
ωB97X-D//cc-pVTZ	3	41
ωB97X-D/aug-cc-pVTZ/ωB97X-D/cc-pVTZ	5	44
ωB97X-D/cc-pVQZ/ωB97X-D/cc-pVTZ	4	44
MP2//cc-pVTZ	-9	42
CCSD/cc-pVTZ/MP2/cc-pVTZ	12	44
CCSD(T)/cc-pVTZ/MP2/cc-pVTZ	5	—
DLPNO-CCSD(T)/cc-pVTZ/MP2/cc-pVTZ	5 (5)	40 (42)
DLPNO-CCSD(T)/aug-cc-pVTZ/MP2/cc-pVTZ	3 (5)	38 (42)
DLPNO-CCSD(T)/cc-pVQZ/MP2/cc-pVTZ	3	41

Table S1 Energy of *Z*1-PABI relative to *E*1-PABI for different levels of theory. All values include ωB97X-D//cc-pVTZ zero-point energy corrections. DLPNO-CCSD(T) values in parentheses assume the 'tight cutoff' criterion.

Collision cross-section measurements

Measured collision cross-sections (Ω_m) for $E1$ and $Z1$ isomers of PABI were calibrated against literature cross sections (Ω_L) for a series of six tetraalkylammonium cations. An example ATD, obtained from a mixture of PABI and tetraalkylammonium cations with the quadrupole mass filter (QMF) switched on and off, is shown in Fig. S2a. The calibration procedure exploits the relationship between an ion's transit time through the drift region (t_d), its mobility (K), and the temperature-dependent integral collision cross-section [Ω], through the Mason-Schamp equation,[6]

$$K = \frac{3ze}{16N}\sqrt{\frac{2\pi}{\mu k_B T}}\left(\frac{1}{\Omega}\right) = \frac{l^2}{t_d V}. \tag{1}$$

Here, z is the charge of the ion, e is the elementary charge, N is the number density of the buffer gas, μ is the reduced mass of the ion-neutral collision pair, k_B is the Boltzmann constant, T is the effective temperature, l is the length of the drift region, and V is the potential drop across the drift region. In our instrument the measured arrival time of an ion packet, t, is given by:

$$t = t_d + t_{oct} + t_{quad} \tag{2}$$

where t_d, t_{oct}, and t_{quad} are the ion transit times through the drift region (pressure $\approx$6 torr), octupole ion guide (pressure $\approx 2\times10^{-4}$ torr), and quadrupole mass filter (pressure $\approx 10^{-6}$ torr), respectively. Values of t_{oct} and t_{quad} were calculated from instrument parameters (dimensions and electrical potentials of the octupole ion guide and quadrupole mass filter) and are short ($\approx$0.1 ms) compared with t_d. Equation 1 can be rearranged to give a linear relation between collision cross section and $t_d\mu^{-1/2}$,

$$\Omega = A t_d \mu^{-1/2} \tag{3}$$

where the constant A depends on pressure and temperature and is determined by plotting Ω_L of the tetraalkylammonium cations[7,8] against our measured values of $t_d\mu^{-1/2}$ (see Fig. S2b). Once A is determined, Ω_m for the $E1$ and $Z1$ isomers of PABI can be ascertained.

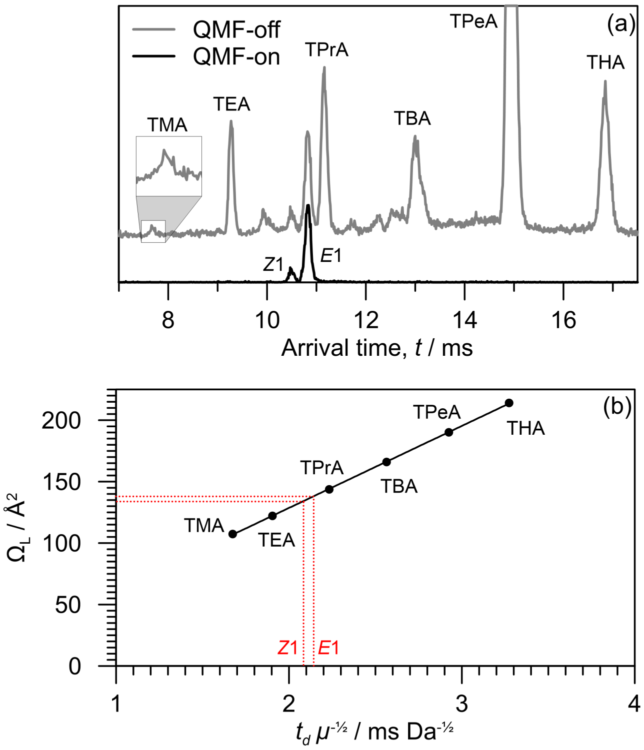

Fig. S2 Collision cross-section calibration for $E1$ and $Z1$-PABI. (a) ATD without mass selection showing $E1$ and $Z1$ PABI peaks and tetraalkylammonium cation peaks (unassigned peaks are solvent adducts). The ATD recorded with mass selection, shows only the $E1$ and $Z1$ PABI peaks. (b) Literature collision cross sections (Ω_L, taken from Refs 7 and 8) for the tetraalkylammonium cations plotted against $t_d\mu^{-1/2}$. TMA= tetramethylammonium, TEA= tetraethylammonium, TPrA= tetrapropylammonium, TBA= tetrabutylammonium, TPeA= tetrapentylammonium, THA= tetrahexylammonium.

Blue light irradiation of PABI solution at pH≈4

As shown in Fig. S3a, irradiation of the PABI solution with 473 nm light from a diode laser leads to net *E*-*Z* photoisomerisation and consequent increase in the relative intensity of the *Z*1 peak in the ATD (0 s trace). In these measurements, following establishment of a photostationary state (PSS) with the blue light, irradiation was ceased and the population of *E*1 and *Z*1 isomers was monitored with ion mobility as a function of time (Fig. S3b).[9] A first order kinetic fit to the decay of the *Z*1-isomer signal in Fig. S3b produced the halflife of $t_{1/2}$=1860±60 s in methanol at pH≈4 (298 K). Weston *et. al.*[1] has shown $t_{1/2}$ to be strongly pH-dependent, varying from 16 s at pH = 9 in methanol to ≈3500 s at pH = 3 in methanol. The strong pH-dependence of $t_{1/2}$ in solution suggests neutral azobis(2-imidazole) has a faster *E*-*Z* thermal reversion rate and isomerisation barrier than PABI. ATDs following irradiation of the pH≈4 solution with 428 nm light gave a *Z*1:*E*1 ratio of 0.4:0.6 (Fig. S3c), to be compared with the ratio of 0.6:0.4 at 473 nm, showing the PSS abundance of *Z*1 to decrease at the shorter wavelength.

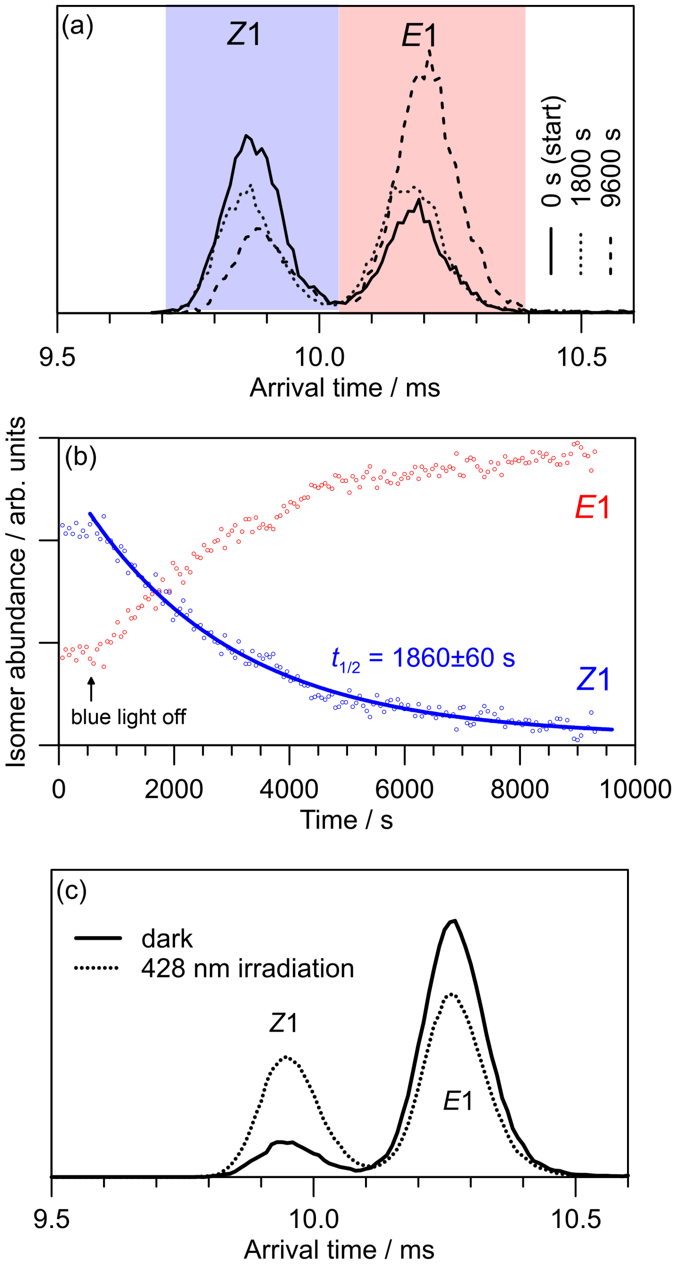

Fig. S3 Blue light irradiation of a pH≈4 solution of PABI in methanol. (a) ATDs recorded with a low RF drive voltage to IF1 at three selected times following establishment of a PSS at 473 nm. (b) Abundance of *E*1 and *Z*1 isomers as a function of time, and a first-order kinetic fit to the *Z*1-isomer abundance. (c) ATDs recorded with a low RF drive voltage to IF1 from a solution shielded from light for several days and following establishment of a PSS at 428 nm.

References

[1] C. E. Weston, R. D. Richardson and M. J. Fuchter, *Chem. Commun.*, 2016, **52**, 4521.

[2] F. Neese, *WIRES Comp. Mol. Sci.*, 2012, **2**, 73.

[3] C. Riplinger, B. Sandhoefer, A. Hansen and F. Neese, *J. Chem. Phys.*, 2013, **139**, 134101.

[4] D. G. Liakos and F. Neese, *J. Chem. Theory Comput.*, 2015, **11**, 4054.

[5] D. G. Liakos, M. Sparta, M. K. Kesharwani, J. M. L. Martin and F. Neese, *J. Chem. Theory Comput.*, 2015, **11**, 1525.

[6] H. E. Revercomb and E. A. Mason, *Anal. Chem.*, 1975, **47**, 970.

[7] I. Campuzano, M. F. Bush, C. V. Robinson, C. Beaumont, K. Richardson, H. Kim and H. I. Kim, *Anal. Chem.*, 2012, **84**, 1026.

[8] J. C. May, C. R. Goodwin, N. M. Lareau, K. L. Leaptrot, C. B. Morris, R. T. Kurulugama, A. Mordehai, C. Klein, W. Barry, E. Darland, G. Overney, K. Imatani, G. C. Stafford, J. C. Fjeldsted and J. A. McLean, *Anal. Chem.*, 2014, **86**, 2107.

[9] J. N. Bull, M. S. Scholz, N. J. A. Coughlan, A. Kawai and E. J. Bieske, *Anal. Chem.*, 2016, **88**, 11978.